Integrative and Comparative Biology Advance Access published April 27, 2015

Integrative and Comparative Biology

Integrative and Comparative Biology, pp. 1–12
doi:10.1093/icb/icv016

Society for Integrative and Comparative Biology

SYMPOSIUM

Hydrodynamics of C-Start Escape Responses of Fish as Studied with Simple Physical Models

William C. Witt,* Li Wen† and George V. Lauder[1,‡]

*Mechanical and Aerospace Engineering, Princeton University, Princeton, NJ 08544, USA; †School of Mechanical Engineering and Automation, Beihang University, Beijing, China 100191; ‡Museum of Comparative Zoology, Harvard University, Cambridge, MA 02138, USA

From the symposium "Unsteady Aquatic Locomotion with Respect to Eco-Design and Mechanics" presented at the annual meeting of the Society for Integrative and Comparative Biology, January 3–7, 2015 at West Palm Beach, Florida.

[1]E-mail: glauder@oeb.harvard.edu

Synopsis One of the most-studied unsteady locomotor behaviors exhibited by fishes is the c-start escape response. Although the kinematics of these responses have been studied extensively and two well-defined kinematic stages have been documented, only a few studies have focused on hydrodynamic patterns generated by fishes executing escape behaviors. Previous work has shown that escape responses by bluegill sunfish generate three distinct vortex rings, each with central orthogonal jet flows, and here we extend this conclusion to two other species: stickleback and mosquitofish. Jet #1 is formed by the tail during Stage 1, and moves in the same direction as Stage-2 movement of the fish, thereby reducing final escape-velocity but also rotating the fish. Jet #2, in contrast, moves approximately opposite to the final direction of the fish's motion and contains the bulk of the total fluid-momentum powering the escape response. Jet #3 forms during Stage 2 in the mid-body region and moves in a direction approximately perpendicular to jets 1 and 2, across the direction of movement of the body. In this study, we used a mechanical controller to impulsively move passively flexible plastic panels of three different stiffnesses in heave, pitch, and heave + pitch motions to study the effects of stiffness on unsteady hydrodynamics of escape. We were able to produce kinematics very similar to those of fish c-starts and also to reproduce the 3-jet hydrodynamic pattern of the c-start using a panel of medium flexural stiffness and the combined heave + pitch motion. This medium-stiffness panel matched the measured stiffness of the near-tail region of fish bodies. This motion also produced positive power when the panel straightened during stage 2 of the escape response. More flexible and stiffer panels resulted in non-biological kinematics and patterns of flow for all motions. The use of simple flexible models with a mechanical controller and program of fish-like motion is a promising approach for studying unsteady behaviors of fish which can be difficult to manipulate experimentally in live animals.

Introduction

The study of unsteady or impulsive locomotor movements in fishes began in earnest with the seminal publications of Weihs (1973) and Webb (1975), and has expanded into a large area of research in recent years. Since the early paper by Sir James Gray (1933) which initiated the study of unsteady locomotor patterns in fishes, the study of rapid escape responses (c-starts or fast-starts) has developed into an active sub-field with a huge literature as researchers interested in the neural control of motion (Eaton 1984; Korn and Faber 1996), those working on the biomechanics of rapid movements (Jayne and Lauder 1993; Domenici and Blake 1997; Wakeling 2006), and investigators interested in comparative behavioral and ecological aspects of animals' escape responses (Webb 1978; Hale et al. 2002; Domenici et al. 2007; Ashley-Ross et al. 2013; Gibb et al. 2013) all focus attention on escape performance by fish (Domenici et al. 2011a, 2011b). A later book edited by Webb and Weihs (1983) entitled "Fish Biomechanics" also played an influential role in stimulating interest in patterns of locomotion in fish.

© The Author 2015. Published by Oxford University Press on behalf of the Society for Integrative and Comparative Biology. All rights reserved. For permissions please email: journals.permissions@oup.com.

Downloaded from http://icb.oxfordjournals.org/ by guest on April 28, 2015

Despite the large literature on the escape responses of fish, impulsive movements in general and escape responses in particular are poorly understood from a hydrodynamic perspective. One paper has investigated experimentally the flow-fields produced by escaping fish (Tytell and Lauder 2008), Epps and Techet (2007) studied the hydrodynamics of unsteady maneuvering in fish, and Read et al. (2003) described impulsive heaving and pitching in a rigid airfoil. Computational analyses of escape responses in fish are just beginning to appear (Borazjani et al. 2012; Borazjani 2013; Li et al. 2014). Flow-fields produced during impulsive movements are of interest due to their possible use by predators in tracking the trajectory of escaping prey (Hanke et al. 2000; Stewart et al. 2013), and for understanding how unsteady movements of fish transfer momentum to the environment and rapidly generate maneuvering forces.

Studies of impulsive movements in live fish are subject to a number of limitations, chief among which is the difficulty of manipulating individual variables such as body surface area, stiffness, and the velocity and magnitude of body motion (Lauder et al. 2012). Early work by Webb (1977) made an important contribution to this issue by modifying trout fins to study c-starts, and he studied the effect of various amputations of the fins on escape performance. Experimental systems that allow controlled manipulations of impulsive motions, however, are not well developed, and this is an area in which progress might allow a new exploration of escape mechanics in fishes.

One approach that could allow controlled study of escape responses is to use robotic or physical models of fish, and simple physical models have increasingly been used to study fishes' undulatory propulsion (e.g., Alben et al. 2012; Lauder et al. 2012; Lauder et al. 2011a; Quinn et al. 2014a, 2014b; Shelton et al. 2014). More complex fish-like biomimetic systems (Epps et al. 2009; Low et al. 2009; Conte et al. 2010; Tangorra et al. 2011; Esposito et al. 2012; Marchese et al. 2014; Su et al. 2014) also have allowed investigators to study a number of key features of the functional design of fish and to test new approaches for modeling functions involved in fishes' locomotion (Lauder 2015; Lauder and Tangorra 2015).

The overall goal of this article is to use physical models of fishes' bodies that vary in flexibility to determine if the complex hydrodynamics produced by fish during c-starts can be reproduced by a simple model system. More specifically, using flexible rectangular plastic panels as models for fishes' bodies we aim to determine (1) the effects of flexibility on c-start kinematic and hydrodynamic patterns, and (2) the effect that different patterns of panel-motion have on c-start hydrodynamic flows.

Background

The c-start response in fishes is a rapid and unsteady or impulsive behavior that is classically separated into two stages: Stage 1 and Stage 2. During Stage 1, the body bends strongly on one side into a c-shape as both red and white muscle fibers contract (Jayne and Lauder 1993; Wakeling 2006), while in Stage 2 the body bends into a propulsive wave generating thrust to move the fish away from the stimulus that caused the response. A final Stage 3 is sometimes defined as a more variable phase during which the fish maneuvers or glides to a stop at the end of the response (Domenici and Blake 1997; Chadwell et al. 2012a).

While there is a very large literature on fishes' escape kinematics and neural control of movement, there is limited knowledge of the hydrodynamics of their escape responses. Recent experimental hydrodynamic research on c-starts has shown that a complex pattern of flow is produced with three nearly orthogonal vortex rings, each with corresponding central jet momentum flows (Tytell and Lauder 2008). Figure 1A shows this pattern for bluegill sunfish. As bluegill bend into a c-shape, the body generates Jet 1 from the posterior region and tail that directs momentum nearly opposite to the final direction of travel and thus represents energy that opposes the ultimate trajectory of the escape. Jet 2 (Fig. 1A) forms from the rapid c-bend of the body, and generates by far the largest momentum powering the trajectory of escape in Stage 2. Jet 3 forms nearly orthogonal to both Jets 1 and 2 as a result of the bending of the body during Stage 2 and serves a steering function that directs the final trajectory. Computational fluid dynamic calculations by Borazjani et al. (2012), based on three-dimensional kinematics of bluegill, accurately reproduce these three jets.

The unexpectedly complex hydrodynamic pattern associated with escape responses is not unique to bluegill sunfish. Figure 1B shows a two-jet pattern for stickleback, with Jet 3 weak or absent, while mosquitofish produce a clear three-jet pattern during escape (Fig. 1C), very similar to that of bluegill. Stickleback possess relatively stiff bodies due to the series of bony plates along their length, and this increased stiffness, relative to that of bluegill, may be responsible for the differences in the magnitude of

Downloaded from http://icb.oxfordjournals.org/ by guest on April 28, 2015

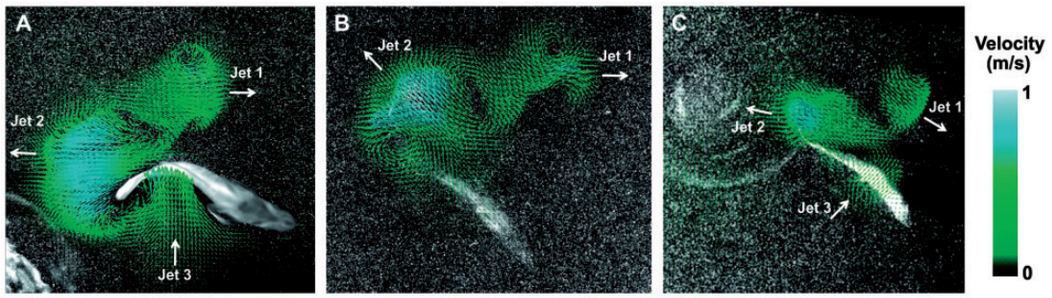

Fig. 1 Patterns of flow observed during c-start escape responses in (**A**) bluegill sunfish (*Lepomis macrochirus;* see Tytell and Lauder 2008), (**B**) Stickleback (*Gasterosteus aculeatus*, Carlson and Lauder, unpublished data), and (**C**) mosquitofish (*Gambusia hubbsi*, Langerhans and Lauder, unpublished data). Each fish generates a jet of fluid and a vortex ring from the caudal region (Jet 1), a large Jet 2 resulting from the c-bend of the body; a Jet 3, orthogonal to the other two jets, is seen in bluegill and mosquitofish. Stickleback generate a very weak Jet 3 not visible in (B). (This figure is available in black and white in print and in color at *Integrative and Comparative Biology* online.)

Jet 3. The study of the stiffness of fish bodies in relation to fluid flow patterns during escape is completely unexplored, and represents a fruitful area for future research.

Materials and methods

In order to study the c-start escape of fishes using flexible panel models (Fig. 2A), we used the same robotic controller developed for studying steady undulatory swimming in fishes (Lauder et al. 2007; Lauder et al. 2011a; Alben et al. 2012; Quinn et al. 2014a; Shelton et al. 2014), but programmed it with impulsive rotational (pitch) and translational (heave) motions (Fig. 2B). This apparatus sits above a water-filled tank or flume and contains motors that allow a shaft 8 mm diameter to be moved in translation and rotation. Encoders provide feedback to the main Labview control program to quantify the motions undergone by the shaft, and an ATI 6-axis force/torque sensor is attached to the shaft and these data are acquired by a Labview program and synchronized with the motion program. All data are sampled at 1000 Hz. A trigger pulse allows simultaneous 1000 frame per second high-speed video (Photron PCI-1024 camera) images of the motion. Flexible panels and rigid foils of various kinds as well as foils covered with fish-skin membranes (e.g., Oeffner and Lauder, 2012) can be attached and moved with this mechanical controller to study their locomotor properties. All trials were conducted in still water.

Experimental data on hydrodynamics were gathered using our standard particle-image velocimetry protocols using 1000 Hz video, and particle-image movies were analyzed using Lavision DaVis software v7.2 (as in Shelton et al. 2014; Standen and Lauder, 2007). We analyzed two-dimensional water-velocity fields from a time series of consecutive video frames (1024 by 1024 pixels) and sequential cross-correlation with an initial interrogation window-size of 64*64 ending at 12*12 (4 passes, overlap 50%). Post-processing of vectors was carried out using a median filter, which removed and iteratively replaced vectors greater than two times the root mean square of their neighbors.

Pitch rotations moved the foil shaft through 60 degrees in 100 ms, while heave motions occurred first in one direction with 1.5 cm amplitude to effect Stage 1, and then in a reverse direction for a distance of 8 cm, which mirrored the Stage-2 and Stage-3 body-motions (Fig. 2B) in the escape responses of fish. These values of pitch and heave were reached after a series of trials which determined that (1) a program of bi-directional heave motion produced a more fish-like c-shape of the flexible panel than did unidirectional motions, and (2) that these motion-program distances and rotation angles and velocities allowed sufficient time for the panels to achieve full bending while still resulting in c-start times that are within the range of those exhibited by live fish.

In order to study the effect of different motion programs on c-start kinematics and hydrodynamics, we used three motion programs: pitch-motion only, heave-motion only, and then a combination of pitch and heave simultaneously. Figure 2 illustrates the positions that one panel took just before the start of impulsive movement (Fig. 2C), during pitch-only motion (Fig. 2D), heave-only motion (Fig. 2E), and with combined heave + pitch (Fig. 2F).

We used flexible plastic panels 12 cm long and 5 cm high, composed of the same material used in our previous work on undulatory propulsion: shim

Downloaded from http://icb.oxfordjournals.org/ by guest on April 28, 2015

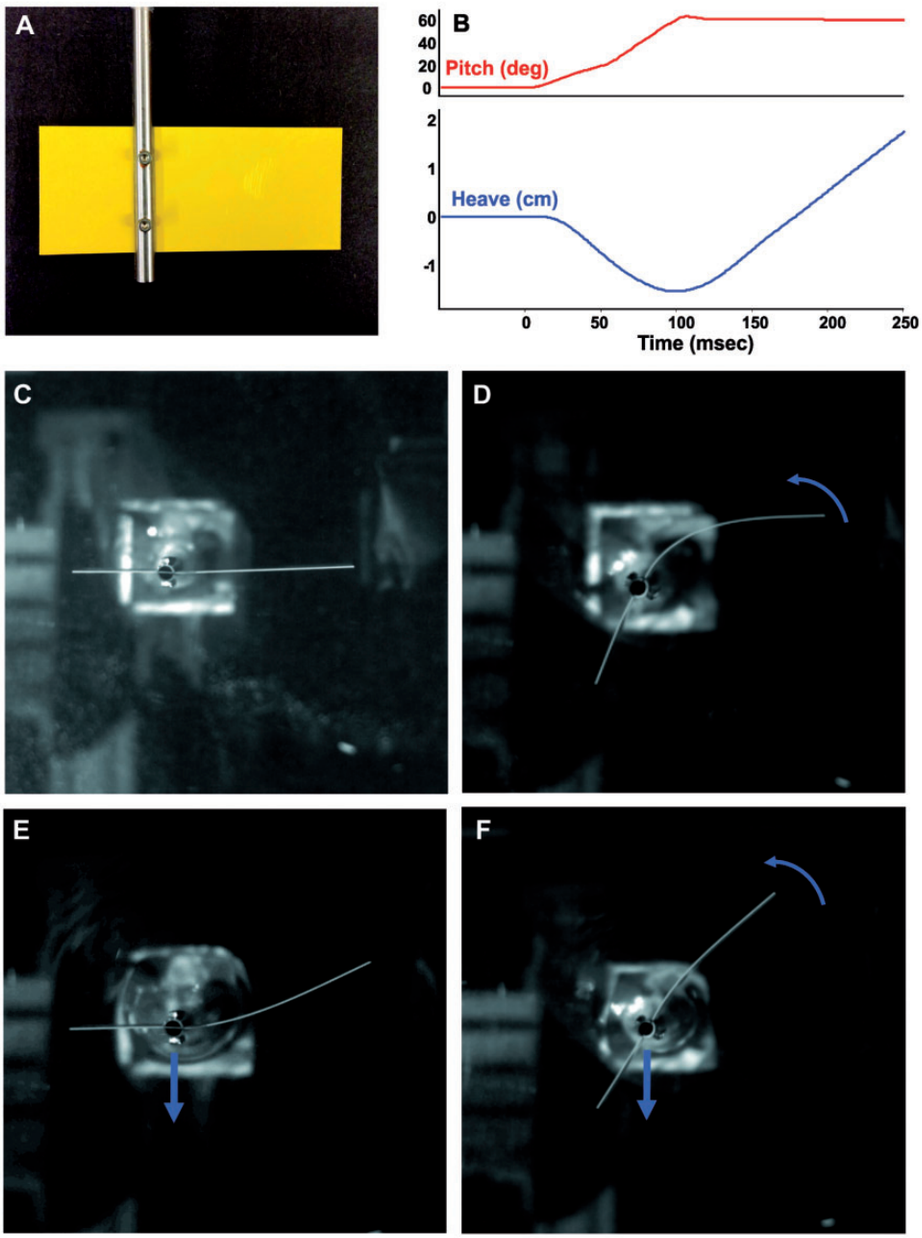

Fig. 2 Physical models of impulsive motion in fish. (**A**) Flexible panel (5 cm by 12 cm) attached to a rod one-third along the length, moved by a robotic controller in rotation (pitch) and translation (heave). (**B**) Program of motion used for both heave and pitch through time (see text for discussion). Heave motion continues at the same rate for a distance of 8 cm. (**C**) Initial position of the panel before start of a program of motion. (**D**) 100 ms into a motion program of pitch only. (**E**) 200 ms into the heave-motion program. (**F**) 140 ms into program of heave + pitch motion. All images shown are from the stiffest foil. Blue arrows schematically show the rotational and translational motions. (This figure is available in black and white in print and in color at *Integrative and Comparative Biology* online.)

stock (ARTUS Corp, Englewood, NJ). These were attached to the controlling rod at the one-third point (Fig. 2A). Panels of three different flexural stiffnesses (EI) were studied: least stiff ($EI = 0.02\,mN^*m^2$), medium stiffness ($EI = 0.31\,mN^*m^2$), and most stiff ($EI = 2.76\,mN^*m^2$). The stiffness of these panels encompasses the range previously reported for the bodies of fish (see Long 1998; McHenry et al. 1995; Shelton et al. 2014).

Center-of-mass (COM) movement trajectories reported here are for the true COM, and not the stretched-straight position of the COM as is often reported when the mass distribution of the bending body is unknown.

Downloaded from http://icb.oxfordjournals.org/ by guest on April 28, 2015

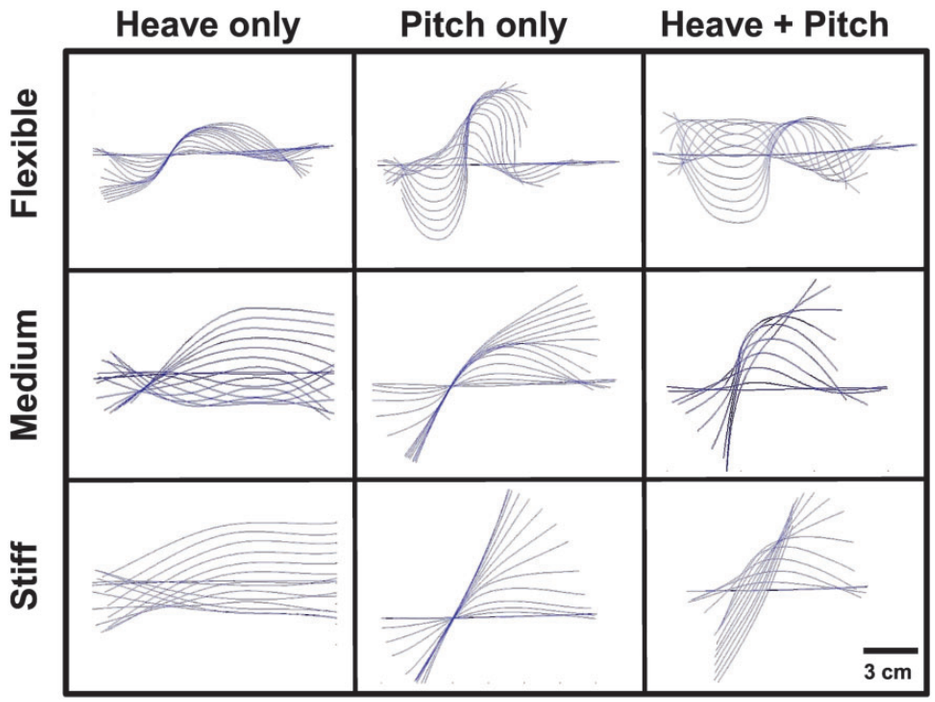

Fig. 3 Midline traces to show the motion of the three flexible panels under each of the three motion programs. See text for discussion. (This figure is available in black and white in print and in color at *Integrative and Comparative Biology* online.)

The experimental plan for this research can be thought of as a three-by-three matrix (see Fig. 3) with materials of three stiffnesses and three motion programs allowing for nine total experimental conditions. Five replicate trials were conducted of each motion program and each material, with a sixth used to collect synchronous data on force and hydrodynamics.

Results

Kinematics of flexible panels

Patterns of movement of the three flexible materials resulting from each of the three motion programs are summarized in Fig. 3. The most flexible panel undergoes considerable bending during all three motions, and no shapes resemble those of fish executing c-starts. The stiffest panel, not surprisingly, tends to maintain its shape throughout each movement pattern, although during the heave + pitch motion there is bending in the longer "tail" region of the panel. The medium-stiffness panel, when moved in heave + pitch, produces body kinematics that closely resemble fish: a c-shape Stage 1, followed by the panel bending into Stage 2, followed by a gliding Stage 3 with the panel held mostly straight. Interestingly, the heave + pitch motion produced a much more pronounced c-shape in this panel than did the heave-motion alone. Although it might be expected that a heave-only motion program might be sufficient to bend the panel into a distinct c-shape, we found that the additional torque contributed by the pitch-motion greatly enhances the extent of the c-shape taken by the panel and enhances the similarity to the Stage 1 pattern of midline bending seen in bluegill sunfish.

Comparison of the midline shapes taken by the medium flexibility panel under the heave + pitch motion with midlines from bluegill escape responses (Fig. 4) show the similarity clearly. Panels and fish are of similar size and both show the initial c-bend followed by Stage 2 motion. Comparison of COM motion in the flexible panels (Fig. 5) shows that the heave + pitch motion produced a V-shaped trajectory in which the top of the V occurred at the end of the first heave period. COM motion of the medium flexibility panel has a sharply pointed V-shape with the heave + pitch and relatively straight trajectories before and after reaching maximal initial heave-motion. Motion in heave produced nearly linear trajectories for all but the most flexible panel in which high curvatures generated a V-shaped path.

Comparison with the COM path of bluegill sunfish during c-starts (Fig. 5) shows that fish exhibit

Downloaded from http://icb.oxfordjournals.org/ by guest on April 28, 2015

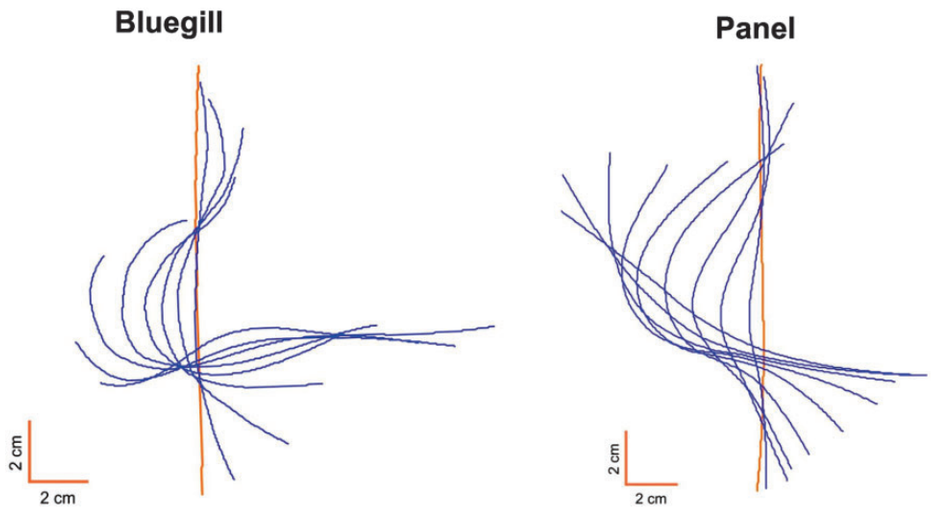

Fig. 4 Comparison of midline traces (blue lines) during the c-start escape response in bluegill sunfish (left) with the medium flexibility panel moved in the heave + pitch motion (right). Red midline indicates the starting position. (This figure is available in black and white in print and in color at *Integrative and Comparative Biology* online.)

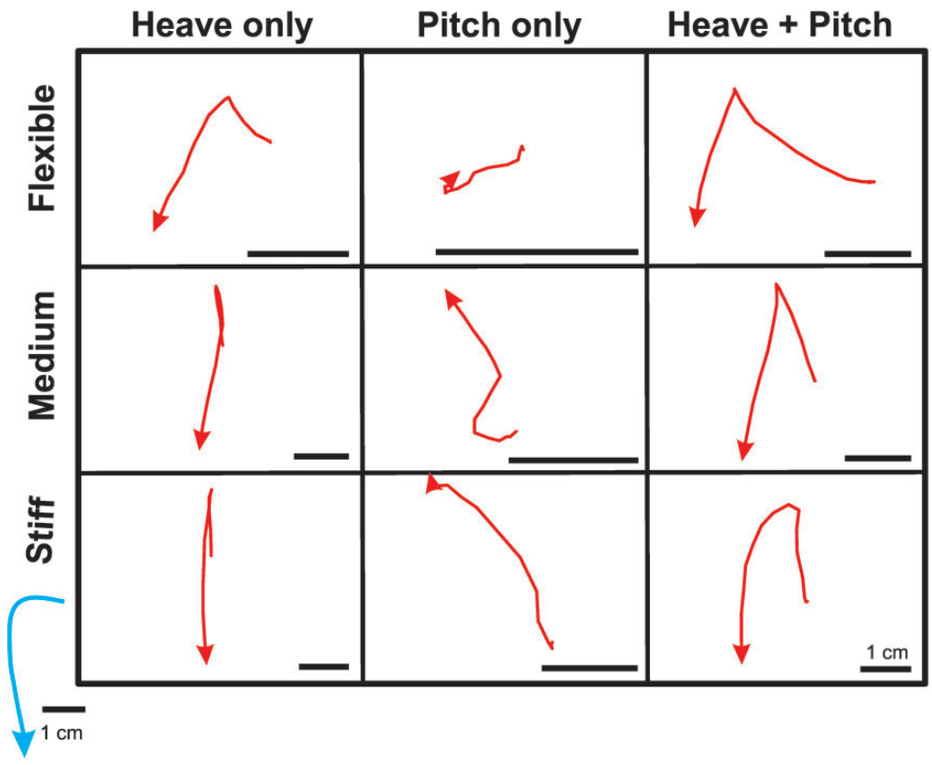

Fig. 5 COM trajectories during impulsive movements by flexible panels of three stiffnesses under each of the three motion programs. Black bars represent 1 cm in all panels; note the differing scales in each panel. The blue COM-trajectory and scale in the lower left is for bluegill's c-starts (modified from Tytell and Lauder 2008). (This figure is available in black and white in print and in color at *Integrative and Comparative Biology* online.)

more of an L-shaped pattern than any flexible panel. Stage 1 in bluegill does not result in significant COM motion in the reverse direction to the final trajectory, unlike the paths resulting from the heave + pitch in the flexible panels.

Hydrodynamics of flexible panels

Particle image velocimetry of each of the three panels undergoing the three different motion programs reveals how the flow patterns associated with each flexibility develop. Heave + pitch produced the most

Downloaded from http://icb.oxfordjournals.org/ by guest on April 28, 2015

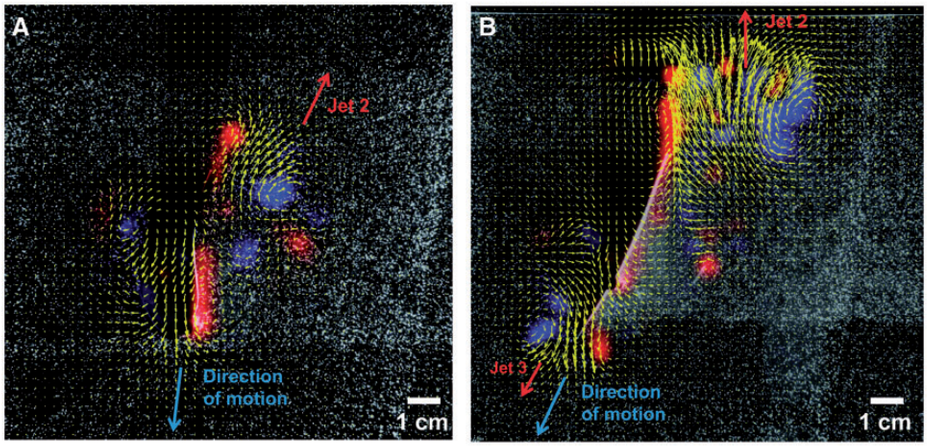

Fig. 6 Particle image velocimetry analysis of the heave + pitch motion in the most flexible panel (**A**) and the stiffest panel (**B**). Images show the flow field at the end of the motion program. Yellow arrows are velocity-vectors; background color indicates clockwise vorticity (blue) and counterclockwise rotation (red). The most flexible panel generates little net momentum as jets of fluid are evident both opposing the direction of motion and opposite to the panel's motion (jet 2). This flow-pattern does not resemble the escape response of fish. The stiffest panel generates a substantial, main-momentum jet but not jet #1 from the "tail" and jet 3 is reoriented to oppose the direction of travel. (This figure is available in black and white in print and in color at *Integrative and Comparative Biology* online.)

fish-like flow patterns and so we concentrate on those here. Figure 6 compares the flow pattern that resulted from the heave + pitch motion of the most flexible and stiffest panel materials. For the most flexible panel (Fig. 6A), there is little net momentum evident at the end of the program. No Jet 1 is visible, and although a Jet 2 results from the c-bend during Stage 1, there is also an opposing flow near the "head" that acts opposite to Jet 2 that could be a modified Jet 3 resulting from bending of the flexible panel during Stage 2. The stiffest panel displays a strong Jet 2, but lacks Jet 1 (Fig. 6B). Jet 3 can be detected, but it is stronger than that of the most flexible panel and also oriented in a direction opposite to the direction of motion and thus would oppose the escape response.

The medium-flexibility panel moved in heave + pitch shows a hydrodynamic pattern that is very much like that of bluegill (Fig. 7). A well-developed Jet 1 is present that has a fish-like orientation. As in bluegill (Fig. 1A), Jet 1 develops from the tail and posterior third of the body and is oriented opposite to the final trajectory. A strong fish-like Jet 2 develops as a result of the panel bending into a C-shape, and a fish-like shear-layer develops between the opposing directional flows of Jets 1 and 2. Jet 3 is oriented perpendicular to the final trajectory, as in bluegill. This combination of flexibility and motion of the panel generates hydrodynamic flows that closely resemble those of live fish executing c-starts.

The in-shaft force/torque sensor allows for measurement of the forces and torques at the shaft of the panel simultaneously with high-speed video of

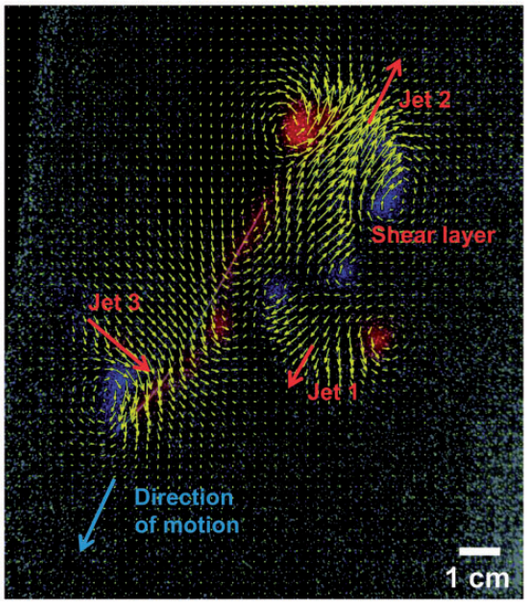

Fig. 7 Analysis of particle-image velocimetry of the heave + pitch motion in the medium-flexibility panel. Images show the field of flow at the end of the motion program. Yellow arrows are velocity-vectors; background color indicates clockwise vorticity (blue) and counterclockwise rotation (red). This panel and the program of heave + pitch motion produce a field of flow that closely resembles the escape response of fish. The three fish-like momentum jets are evident as is the shear-layer between jet #1 and jet #2.

patterns of the flow and of bending of the panel. As one would expect, the reaction-force increases as the C-bend develops (Fig. 8: positive Y-direction force before 50 ms) and the torque on the shaft

Downloaded from http://icb.oxfordjournals.org/ by guest on April 28, 2015

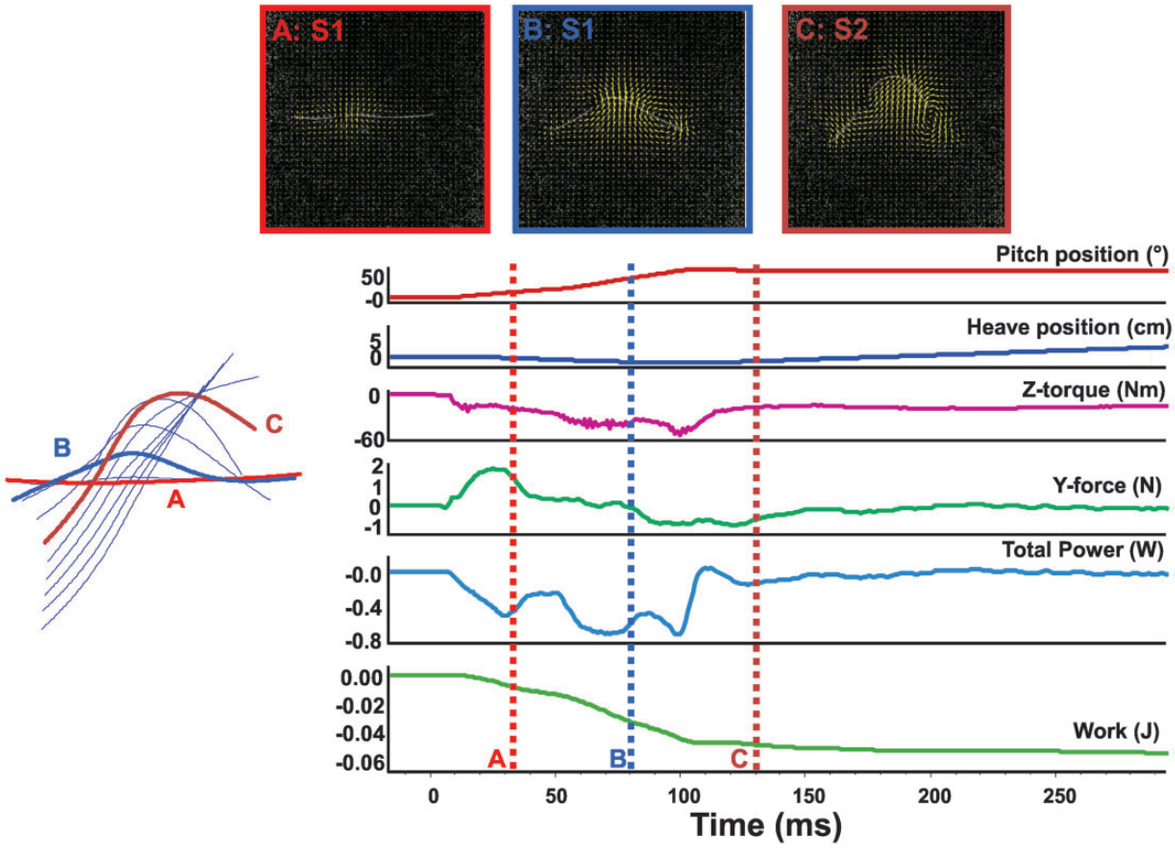

Fig. 8 Graph of the pitch-and-heave-motion program and selected forces and torques recorded from the shaft holding the medium-flexibility panel during heave + pitch motion. Negative work indicates that the driving motors are doing work on the panel. Midlines of the foil and corresponding fluid flow patterns are shown for three times during the motion program (A, B, and C); positive Y is toward the bottom of each panel, positive X is to the left, and positive Z comes out of the page. Times A and B occur during Stage 1, the initial C-bend, while time C is during Stage 2 when the panel straightens out into the propulsive phase. (This figure is available in black and white in print and in color at *Integrative and Comparative Biology* online.)

generally increases throughout Stage 1 (as rotation of the panel imposes torques) and Stage 2 (as translation of the shaft begins and the asymmetrical panel generates moments around the shaft): negative Z-direction torque (Fig. 8).

Total power (Fig. 8), the sum of the instantaneous heave-power (force multiplied by linear velocity) and pitch-power (torque multiplied by angular velocity), shows a biphasic pattern that returns to near baseline shortly after the end of Stage 1. The sensor was oriented such that negative values of power indicate moments when the upper shaft is actively working to move the panel through the water (i.e., the panel-fluid system is resisting the imposed motion). Conversely, positive power indicates times in which the upper shaft works instead to restrain the panel (i.e., the panel-fluid system would tend to propel the panel along its course if detached from the rod).

We observed that when the medium-flexibility panel was moved in heave + pitch, there were two times when the power-curve became positive. This indicates that the moving panel was transmitting positive force to the shaft (where positive means along the prescribed path of motion), whereas at all other times the panel tended to resist the motion imposed by the motors above (Fig. 9). This condition was never observed for any other program of flexibility or motion of the panel: only for the flexibility and motion that also produced the fish-like c-start hydrodynamic pattern.

The first time (Fig. 9: 1, about 100 ms) that the power-curve becomes positive, the panel is decelerating before reversing the direction of heave and we attribute this spike in power to the acceleration reaction caused by decelerating water pressing against the panel and reducing the power needed by the motors during this part of Stage 1. Moreover, this first spike is an artifact of the un-fish-like V-shaped COM trajectory discussed in the previous section. The second positive period

Downloaded from http://icb.oxfordjournals.org/ by guest on April 28, 2015

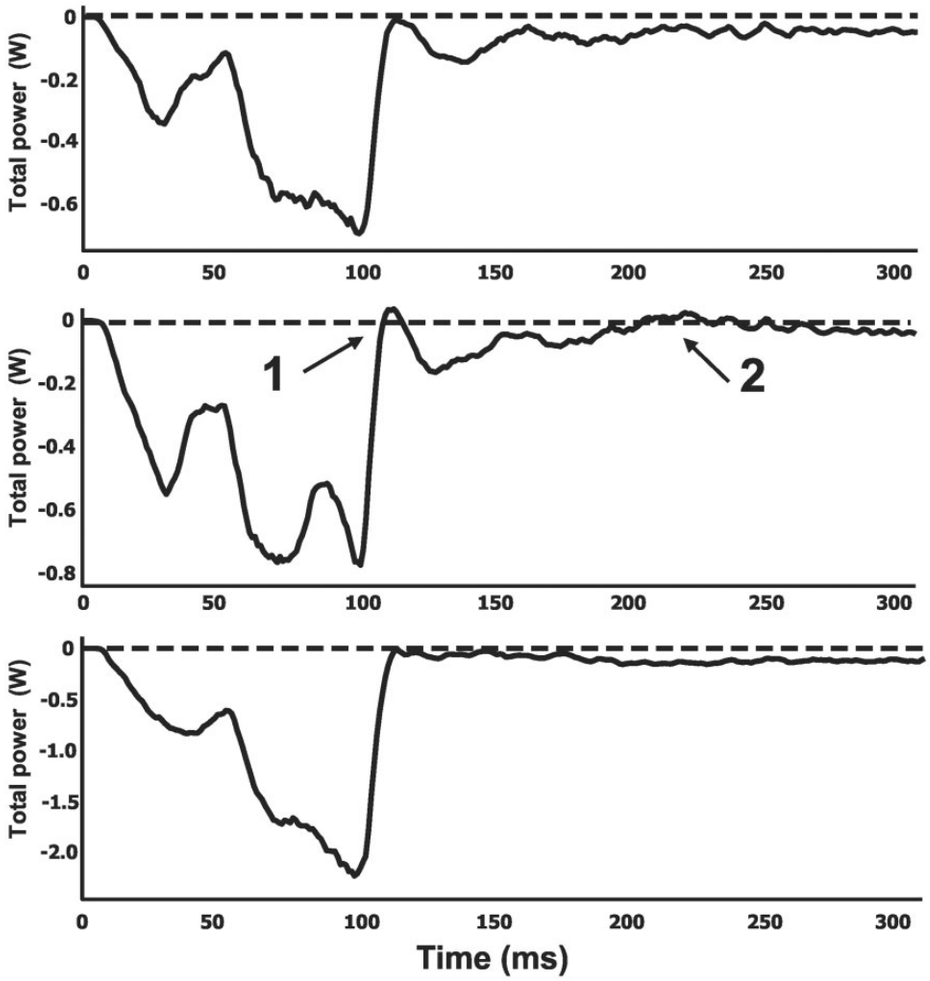

Fig. 9 Graph of the total power versus time for the medium-flexibility panel during programs of pitch-only motion (top), heave + pitch motion (middle), and the heave-only motion (bottom). Negative values indicate that the driving motors are putting power into the panel to overcome hydrodynamic opposition to motion (i.e., drag and related forces). Only the medium-flexibility panel shows any positive power, and two different times (1 and 2) are shown where this occurs, indicating periods when hydrodynamic forces are tending to propel the panel along its path rather than opposite to it. See text for further discussion.

(Fig. 9: 2, around 220 ms) occurs later in the motion program when the panel is springing back toward a straight configuration after having been bent by earlier pitch and heave. We attribute this peak in power to the flexural stiffness of the medium panel and the pattern of flow set up by prior motions—namely the creation of a sufficiently strong Jet 2 to engender a brief period of propulsion—mimicking the burst obtained from a c-start.

Discussion

Simple panel models of c-starts

While the use of simple, flexible panels is an obvious oversimplification of the morphology of fish, working with physical models and a robotic controller does allow manipulation of key parameters such as rotational and translational movements and flexural stiffness that are not amenable to alteration in live fishes. Comparative studies of fish locomotor patterns are necessarily uncontrolled, with many possible factors such as differences among species in the structure of the circulatory system, body musculature, and skeleton all confounding possible causal interpretations of the relationship between the shape of the body and the kinematic patterns (Lauder et al. 2012). Furthermore, differences observed between one of the simplest possible models for a moving fish and the patterns of flow around live fish may be informative as to the causes of these patterns. The ability to measure forces and torques through time at high resolution on moving panels allows measurement of parameters and the design of experiments that are not easily possible with

Downloaded from http://icb.oxfordjournals.org/ by guest on April 28, 2015

swimming animals or freely swimming mechanical devices.

We believe that this is the first study involving the use of a mechanical device that allows controlled manipulation of a physical model to mimic rapid maneuvers of fish. Our results showed that the combination of a panel with medium flexibility, held at the one-third length, and a program of motion that involves both rotation and translation, permits remarkably accurate production of bending patterns and hydrodynamic flows observed in live fish. Also, our medium-flexibility panel generally matches the material characteristics of the mid-body region of swimming fish (see Lauder et al. 2011b; Shelton et al. 2014). In addition, we showed that for certain times in the motion program, the flexible panel can do work on the motors. Flexibility of the panel and the timing of translational and rotational motion both are key to generating a fish-like hydrodynamic wake. In particular, the bidirectional program of heave motion generated panel-bending patterns that were much more fish-like and produced substantially greater curvature than did unidirectional motions alone. In addition, we noticed that adding the rotational component of panel motion, beginning during the initial 1.5 cm heave motion, greatly enhanced the bending observed in the flexible panels and also contributed to the fish-like hydrodynamic wake. Moving the panels sequentially, first in heave, and only later in pitch, generated non-fish-like patterns of wake flow. Exploration of changing the phase relationships between heave and pitch would be a fruitful area for future work.

Despite these similarities between the medium-flexibility panel and fish's c-start patterns, there are two key differences. First, the COM patterns differ (Fig. 4: compare the blue trace in the lower left with the red traces showing panel COM motion). The panels were moved in a bidirectional heave-pattern which deflects the COM initially to one side before starting movement back along the final trajectory of Stage 2. Bluegill sunfish do not show this initial deflection of the COM, and we believe that this is due to active bending of the fish's body by red and white body musculature that allows fish to bend into a c-shape with minimal displacement of the COM. In order to generate the c-bend with our flexible panels, we moved the actuator first in one direction, and then back in another, and this necessarily displaces the COM. Although this pattern of motion still allowed a hydrodynamic c-start pattern that was remarkably similar to that of fish, we expect that development of more realistic models of fish would generate more accurate COM tracks. Second, motor power limited the speed to which we could impose rotations and translations on the shaft of the panel. This resulted in longer duration of responses from the panels compared to live-fish c-starts which can be quite rapid and are often completed within 100 ms. The panel-motions resulting from the heave + pitch program were well established along the final trajectory by 200 ms, but this is still longer than the c-start behavior would take in bluegill sunfish (Jayne and Lauder 1993; Chadwell et al. 2012a, 2012b; Tytell and Lauder 2008).

A final important difference between fish-bodies and panels concerns the uniform flexibility of the panels used here. While using simple, uniformly-stiff panels held at the one-third position to produce a shorter "head" and longer "tail" is a reasonable first step, fish clearly have non-uniform bodies that vary in surface area, mass, and material properties along the body. Exploring the effect of non-uniform stiffness on impulsive movements will be an important next step toward better understanding the effects of the shape of the body and the distribution of mass on maneuvering behaviors. Research certainly could begin with passive models that possess the mechanical properties of the bodies of fish.

Working with fish-like models

Although we have focused here on using physical models to better understand rapid, unsteady movements with simple, flexible panels, future work could involve more sophisticated fish-like systems that can mimic various aspects of impulsive fish behavior. One method that combines some of the features of the simplified approach used here with a mechanism that allows more rapid accelerations similar to those of fish, is the device used by Conte et al. (2010). They designed a fish-like model (a metal beam covered in urethane rubber), bent it into a c-shape, and held the model in that shape with a restraining line. This line was then cut and the model rapidly straightened with resulting accelerations and forward propulsion. Conte et al. (2010) observed high accelerations, although still not at the magnitudes reported in current literature on the c-start responses of fish. One disadvantage of this mechanism is that it is not easy to alter the motion program of the body once it is released, or to introduce more complex motions with distinct Stage-1 and Stage-2 components.

Marchese et al. (2014) designed an autonomous robotic fish made from silicone elastomer and controlled by an internal pneumatic cylinder and valves to generate locomotor movements similar to those of

Downloaded from http://icb.oxfordjournals.org/ by guest on April 28, 2015

live fish. Their model produced similar patterns of bending of the body to that of a fish's c-start, although the time-course was much longer. Stage-1 movements by this model fish lasted approximately 550 ms, while in bluegill studied by Tytell and Lauder (2008) the mean duration of Stage 1 was 35 ms. Scaling effects could certainly account for some of the longer durations of movement, as the model fish of Marchese et al. (2014) was nearly 35 cm in total length, compared to the bluegill sunfish's mean length of 11 cm. Su et al. (2014) designed a multi-joint robotic fish that executed a c-start-like behavior with a turning rate of up to 670 deg/sec in 200 ms.

Learning from both simpler and more complex robotic systems will be important in future studies of modes of unsteady swimming in fishes, as manipulation both of motion and of temporal variables will be critical for a better understanding of the factors that control the production of hydrodynamic force. While there are certainly challenges associated with building and controlling more complex devices, we believe that using physical models of all kinds to understand unsteady behavior of fish will be of increasing importance in the future.

Acknowledgments

The authors thank members of the Lauder Laboratory for their invaluable assistance with this research, and Drs Eric Tytell, Iman Borazjani, Rose Carlson, and Brian Langerhans for collaborative work on bluegill, stickleback, and *Gambusia* c-starts.

Funding

This work was supported by the Office of Naval Research ONR-MURI [N000141410533] monitored by Dr Bob Brizzolara, ONR [N00014-09-1-0352] monitored by Dr Tom McKenna, and by National Science Foundation [EFRI-0938043] and [CDI 0941674].

References

Alben S, Witt C, Baker TV, Anderson EJ, Lauder GV. 2012. Dynamics of freely swimming flexible foils. Phys Fluids 24: 051901.

Ashley-Ross MA, Perlman BM, Gibb AC. 2013. Jumping sans legs: does elastic energy storage by the vertebral column power terrestrial jumps in bony fishes? Zoology 117:7–18.

Borazjani I. 2013. The functional role of caudal and anal/dorsal fins during the c-start of a bluegill sunfish. J Exp Biol 216:1658–69.

Borazjani I, Sotiropoulos F, Tytell ED, Lauder GV. 2012. On the hydrodynamics of the bluegill sunfish c-start escape response: three-dimensional simulations and comparison with experimental data. J Exp Biol 215:671–84.

Chadwell BA, Standen EM, Lauder GV, Ashley-Ross MA. 2012a. Median fin function during the escape response of bluegill sunfish (*Lepomis macrochirus*). I: fin-ray orientation and movement. J Exp Biol 215:2869–80.

Chadwell BA, Standen EM, Lauder GV, Ashley-Ross MA. 2012b. Median fin function during the escape response of bluegill sunfish (*Lepomis macrochirus*). II: fin-ray curvature. J Exp Biol 215:2881–90.

Conte J, Modarres-Sadeghi Y, Watts MN, Hover FS, Triantafyllou MS. 2010. A fast-starting mechanical fish that accelerates at 40 m s −2. Bioinsp Biomimet 5:035004.

Domenici P, Blagburn JM, Bacon JP. 2011a. Animal escapology I: theoretical issues and emerging trends in escape trajectories. J Exp Biol 214:2463–73.

Domenici P, Blagburn JM, Bacon JP. 2011b. Animal escapology II: escape trajectory case studies. J Exp Biol 214:2474–94.

Domenici P, Blake RW. 1997. The kinematics and performance of fish fast-start swimming. J Exp Biol 200:1165–78.

Domenici P, Claireaux G, McKenzie DJ. 2007. Environmental constraints upon locomotion and predator–prey interactions in aquatic organisms: an introduction. Phil Trans R Soc Lond B 362:1929–36.

Eaton RC. 1984. Neural mechanisms of startle behavior. New York: Plenum Press.

Epps B, Techet A. 2007. Impulse generated during unsteady maneuvering of swimming fish. Exp Fluids 43:691–700.

Epps B, Valdivia y Alvarado P, Youcef-Toumi K, Techet A. 2009. Swimming performance of a biomimetic compliant fish-like robot. Exp Fluids 47:927–39.

Esposito C, Tangorra J, Flammang BE, Lauder GV. 2012. A robotic fish caudal fin: effects of stiffness and motor program on locomotor performance. J Exp Biol 215:56–67.

Gibb AC, Ashley-Ross MA, Hsieh ST. 2013. Thrash, flip, or jump: the behavioral and functional continuum of terrestrial locomotion in teleost fishes. Int Comp Biol 53:295–306.

Gray J. 1933. Directional control of fish movement. Proceedings of the Royal Society of London Series B, Containing Papers of a Biological Character. p. 115–25.

Hale M, Long J, McHenry MJ, Westneat M. 2002. Evolution of behavior and neural control of the fast-start escape response. Evol 56:993–1007.

Hanke W, Brucker C, Bleckmann H. 2000. The ageing of the low-frequency water disturbances caused by swimming goldfish and its possible relevance to prey detection. J Exp Biol 203: 1193–200.

Jayne BC, Lauder GV. 1993. Red and white muscle activity and kinematics of the escape response of the bluegill sunfish during swimming. J Comp Physiol A 173: 495–508.

Korn H, Faber DS. 1996. Escape behavior – brainstem and spinal cord circuitry and function. Curr Opin Neurobiol 6: 826–32.

Lauder GV. 2015. Fish locomotion: recent advances and new directions. Ann Rev Marine Sci 7: 521–45.

Lauder GV, Anderson EJ, Tangorra J, Madden PGA. 2007. Fish biorobotics: kinematics and hydrodynamics of self-propulsion. J Exp Biol 210: 2767–80.

Lauder GV, Flammang BE, Alben S. 2012. Passive robotic models of propulsion by the bodies and caudal fins of fish. Int Comp Biol 52: 576–87.

Lauder GV, Lim J, Shelton R, Witt C, Anderson EJ, Tangorra J. 2011a. Robotic models for studying undulatory locomotion in fishes. Marine Tech Soc J 45: 41–55.

Downloaded from http://icb.oxfordjournals.org/ by guest on April 28, 2015

Lauder GV, Madden PGA, Tangorra J, Anderson E, Baker TV. 2011b. Bioinspiration from fish for smart material design and function. Smart Mater Struct 20: doi:10.1088/0964-1726/20/9/094014.

Lauder GV, Tangorra JL. 2015. Fish locomotion: biology and robotics of body and fin-based movements. In: Du R, Li Z, Youcef Toumi K, Valdivia P, Alvarado Y, editors. Robot fish – bio-inspired fishlike underwater robots. Beijing, China: Springer Verlag.

Li G, Müller UK, van Leeuwen JL, Liu H. 2014. Escape trajectories are deflected when fish larvae intercept their own c-start wake. J Roy Soc Inter 11: 20140848.

Long J. 1998. Muscles, elastic energy, and the dynamics of body stiffness in swimming eels. Amer Zool 38: 771–92.

Low KH, Zhou C, Zhong Y. 2009. Gait planning for steady swimming control of biomimetic fish robots. Adv Robotics 23: 805–29.

Marchese AD, Onal CD, Rus D. 2014. Autonomous soft robotic fish capable of escape maneuvers using fluidic elastomer actuators. Soft Robotics 1: 75–87.

McHenry MJ, Pell CA, Long JA. 1995. Mechanical control of swimming speed: stiffness and axial wave form in undulating fish models. J Exp Biol 198: 2293–305.

Oeffner J, Lauder GV. 2012. The hydrodynamic function of shark skin and two biomimetic applications. J Exp Biol 215: 785–95.

Quinn DB, Lauder GV, Smits AJ. 2014a. Scaling the propulsive performance of heaving flexible panels. J Fluid Mech 738: 250–67.

Quinn DB, Moored KW, Dewey PA, Smits AJ. 2014b. Unsteady propulsion near a solid boundary. J Fluid Mech 742: 152–70.

Read DA, Hover FS, Triantafyllou MS. 2003. Forces on oscillating foils for propulsion and maneuvering. J Fluid Struct 17: 163–83.

Shelton R, Thornycroft P, Lauder G. 2014. Undulatory locomotion by flexible foils as biomimetic models for understanding fish propulsion. J Exp Biol 217: 2110–20.

Standen EM, Lauder GV. 2007. Hydrodynamic function of dorsal and anal fins in brook trout (*Salvelinus fontinalis*). J Exp Biol 210: 325–39.

Stewart WJ, Cardenas GS, McHenry MJ. 2013. Zebrafish larvae evade predators by sensing water flow. J Exp Biol 216: 388–98.

Su Z, Yu J, Tan M, Zhang J. 2013. Implementing flexible and fast turning maneuvers of a multijoint robotic fish. IEEE/ASME Trans Mech 99: 1–10.

Tangorra J, Phelan C, Esposito C, Lauder G. 2011. Use of biorobotic models of highly deformable fins for studying the mechanics and control of fin forces in fishes. Int Comp Biol 51: 176–89.

Tytell ED, Lauder GV. 2008. Hydrodynamics of the escape response in bluegill sunfish, *Lepomis macrochirus*. J Exp Biol 211: 3359–69.

Wakeling JM. 2006. Fast-start mechanics. In: Shadwick RE, Lauder GV, editors. Volume 23 in Fish Physiology. San Diego: Academic Press. p. 333–68.

Webb PW. 1975. Acceleration peformance of rainbow trout *Salmo gairdneri* and green sunfish *Lepomis cyanellus*. J Exp Biol 63: 451–65.

Webb PW. 1977. Effects of median fin amputation on fast-start performance of rainbow trout (*Salmo gairdneri*). J Exp Biol 68: 123–35.

Webb PW. 1978. Fast start performance and body form in seven species of teleost fish. J Exp Biol 74: 211–16.

Webb PW, Weihs D. 1983. Fish biomechanics. New York: Praeger Publishers.

Weihs D. 1973. The mechanism of rapid starting of slender fish. Biorehology 10: 343–50.

Downloaded from http://icb.oxfordjournals.org/ by guest on April 28, 2015